The Journal of Physical Chemistry Letters

Chemical and Dynamical Processes in Solution; Polymers, Glasses, and Soft Matter

Asymmetric Composition of Ionic Aggregates and the Origin of High Correlated Transference Number in Water-In-Salt Electrolytes

Zhou Yu, Larry A Curtiss, Randall E. Winans, Y Z, Tao Li, and Lei Cheng

J. Phys. Chem. Lett., **Just Accepted Manuscript** • DOI: 10.1021/acs.jpclett.9b03495 • Publication Date (Web): 17 Jan 2020

is published by the American Chemical Society. 1155 Sixteenth Street N.W., Washington, DC 20036

Asymmetric Composition of Ionic Aggregates and the Origin of High Correlated Transference Number in Water-in-Salt Electrolytes

Zhou Yu[1], Larry A. Curtiss[1*], Randall E. Winans[2], Yang Zhang[3], Tao Li[2,4*], Lei Cheng[1*]

[1]Materials Science Division and Joint Center for Energy Storage Research, Argonne National Laboratory, Lemont, Illinois 60439, USA
[2]X-ray Science Division, Argonne National Laboratory, Lemont, Illinois 60439, USA
[3]Department of Nuclear, Plasma, and Radiological Engineering, Beckman Institute for Advanced Science and Technology, Program of Computational Science and Engineering and Department of Electrical and Computer Engineering, University of Illinois at Urbana–Champaign, Urbana, Illinois 61801, USA
[4]Department of Chemistry and Biochemistry, Northern Illinois University, DeKalb, Illinois 60115, USA

*curtiss@anl.gov, tli4@niu.edu, leicheng@anl.gov

Abstract

The "water-in-salt" electrolytes open up exciting new avenues for expanding the electrochemical window of aqueous electrolytes. In this work, we investigated the solvation structure and dynamics of highly concentrated lithium bis(trifluoromethane)sulfonimide aqueous electrolyte using experimentally corroborated molecular dynamics simulations. The simulations revealed the heterogeneous structure of the electrolyte comprises percolating networks of ion and water domains/aggregates. Interestingly, the ionic regions are composed of more $TFSI^-$ ions than Li^+ ions. The Li^+ ion transport mechanism was further explored. Li^+ ions can hop along the coordinated $TFSI^-$ ions in the ionic aggregates. The calculated correlated transference number of the 20 m electrolyte is ~0.32, reasonably high for the high concentration due to a weak negative correlation between the motion of cations and anions within the heterogeneous microscopic domains. These MD results connect the heterogeneous structure of the electrolyte with the correlated dynamics of the Li^+ ion and provide a new understanding of the Li^+ ion transport mechanism in this novel electrolyte.

Keywords: Water-in-salt electrolytes, ionic aggregate, correlated transference number, molecular dynamics

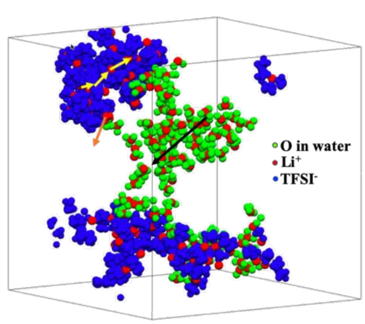

Liquid electrolytes (e.g., aqueous electrolytes, organic electrolytes, and ionic liquids) have broad applications in batteries due to their high ionic conductivity and negligible volume change during a charge/discharge process.[1, 2] Compared to the organic electrolytes and ionic liquids, aqueous electrolytes typically exhibit higher ionic conductivity, intrinsic safety, and are potentially low-cost. However, traditional aqueous electrolytes with a salt concentration lower than 5 m have a voltage window of ~1.2 V due to the electrolysis of water, limiting their applications in high-voltage batteries.[3, 4] Recent breakthrough work from Xu's group reported a highly concentrated 21 m LiTFSI aqueous electrolyte[5] with exceptional performance in a Lithium-ion battery (LIB). It has a wide electrochemical window (~3.0 V) and high stability (nearly 100% coulombic efficiency cycled up to 1000 times at 2.3 V at both low (0.15 C) and high (4.5 C) discharge and charge rates), which is comparable to the commercial LIB with an organic liquid electrolyte.[5] Inspired by this seminal work, other water-in-salt electrolytes (WiSE) have been investigated for sodium-ion and potassium-ion batteries. These studies also showed significantly improved electrochemical performances of WiSE compared to the traditional dilute aqueous electrolytes.[6, 7]

Several investigations using molecular dynamics (MD) simulations have advanced our understanding of the structure and dynamics of the highly concentrated LiTFSI aqueous electrolytes. Borodin et al. have found the inhomogeneous distribution of Li^+ ion.[8] The diffusion of water-separated Li^+ ions in the bulk-like water domains contributes to the high conductivity and transference number.[8] Using combined MD and femtosecond IR studies, Cho et al. have captured the existence of nanometric water channels and interfacial water on ion aggregates in the highly concentrated electrolyte.[9] Furthermore, the unexpected high conductivity of Li^+ ion originates from the percolated bulk-like water channels.[9] These studies presented a similar general observation that the distribution of salt and water is heterogeneous in WiSE systems and watersolvated Li^+ ions preferably move through the bulk-like water domain. However, the majority of ions in the highly concentrated LiTFSI aqueous electrolytes form ionic aggregates. The structure and dynamics of ions in the aggregates cannot be simply extrapolated from prior investigations.

In this work, we studied the LiTFSI aqueous electrolyte using MD simulations with experimental validation. Key results include (1) the observation of the asymmetric composition of ionic aggregates, (2) the existence of two diffusion mechanisms of Li^+ ions in the ionic aggregate, and (3) an explanation for the structural origin of the highly correlated transference number in WiSE systems. The number of Li^+, $TFSI^-$, and water is chosen to set up MD simulations with different nominal concentrations (e.g., 5, 10, 15, and 20 m). The force fields for the Li^+ and $TFSI^-$ ion were taken from previously published work[10, 11], which were developed and optimized within the framework of the OPLS-aa force field.[12] The TIP3P model was employed for the water molecules.[13] A two-stage equilibrium simulation was performed under the NPT and NVT ensemble. For NPT equilibrium simulation, the pressure and temperature were maintained at 1 atm and 298 K. Box size and system energy were stable after a 30 ns simulation. For NVT equilibrium simulation, the coordination environment of Li^+ ion including the coordination number of water and $TFSI^-$ ion were stable after a 50 ns simulation. Finally, a 250 ns production simulation was performed under the NVT ensemble. We conducted small angle x-ray scattering (SAXS) experiments to validate the performance of the force field used in MD simulations on the prediction of the macroscopic structure of the highly concentrated LiTFSI aqueous electrolyte. SAXS is a very powerful technique for providing direct size information of nanometer-scale structures such as colloids, porous materials, biomolecules, and proteins.[14] Recently, our SAXS study revealed unexpected aggregation behaviors in mixed carbonate Li-ion electrolytes, demonstrating that such techniques are very useful for uncovering microscopic aggregate structures that have largely been overlooked before in liquid electrolytes.[15]

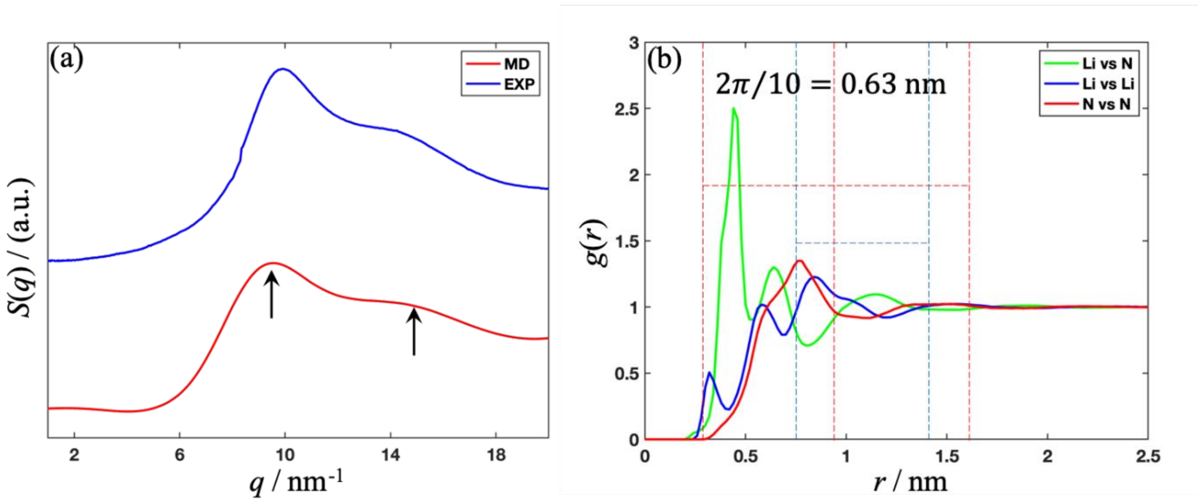

Figure 1. (a) Structure factor calculated using MD simulation (red) and from SAXS experiment (blue) for 20 m LiTFSI aqueous electrolyte. (b) Radial distribution functions (RDFs) from Li^+ ion to the nitrogen atom in $TFSI^-$ ion (green), from Li^+ ion to Li^+ ion (blue), and from nitrogen atom to nitrogen atom in $TFSI^-$ ion (red) for the 20 m electrolyte in MD simulations.The distance beween the same color dashed lines indicate the characteristic wavelength of RDFs, which are related to the position of the corresponding charge ordering peak (COP). The first red dashed line starts at the beginning of the red line. The other red and blue dashed lines locate at the position of $g(r)=1$.

We use SAXS to study 20 m LiTFSI aqueous electrolyte and the result as the blue line in Figure 1a shows two structure factor ($S(q)$) peaks at q = 10 and 15 nm^{-1}. The simulated structure factor calculated using MD (red line in Figure 1a) agrees well with the SAXS results and, thus, justified the reliability of the force field. We further analyzed the MD results to investigate the structural origins that give rise to the SAXS peak features. The peak at ~10 nm^{-1} on the structure factor profile corresponds to the charge ordering peak (COP), which has been widely observed in ionic liquid and molten salts.[16-18] Because ions tend to be surrounded by their counterions to achieve the local electro-neutrality, they form an extended electrostatic network and this leads to this prominent COP peak. The q value of the COP corresponds to a characteristic distance of ~0.63 nm, which is roughly captured in the radial distribution functions (RDFs) shown in Figure 1b.

Specifically, one red or blue peak occurs between two red or blue dashed lines, respectively. One red peak indicates the appearance of one $TFSI^-$ ion layer around the center $TFSI^-$ ion. Similarly, one blue peak represents one Li^+ ion layer around the center Li^+ ion. The characteristic distance is slightly larger than the prior research on the structure factor of the pure LiTFSI liquid,[18] which means the electrostatic network swells when water is added. The peak at ~15.0 nm^{-1} corresponds to the distance between the neighboring atoms of different aions with a distance of ~0.42 nm.[18] Through decoupling the structure factor curve, we found that fluorine-carbon and fluorine-fluorine interaction attributes mainly to the shoulder of the peak (see Fig. S1). This suggests that $TFSI^-$ ions can be fairly close to each other at this concentration and they form aggregate structures (the ionic aggregate). Li^+ ions are also present in these aggregate structures although the contribution of the Li^+ ions to the structure factor is minimum due to the low scattering factor.

Upon further analysis of the ionic aggregate structures from our MD simulations, we found that the solvation features of the concentrated electrolytes are quite different from a dilute solution and the solution species form quite distinct heterogeneous domains. First, we look for bulk-like water in the electrolyte. We use the single-linkage clustering algorithm (see supporting information for details) to define a water cluster. The cutoff distance is 0.38 nm, which corresponds to the first valley in the RDF between oxygen atoms in the water molecules in 1 m (see Fig. S2). A large water cluster would indicate the solvent molecules are connected with each other and thus more "bulk-like", while a small water cluster would indicate that water molecules are in separated micro-domains. Our analysis shows that at 10m and 15m concentrations, the majority of the water molecules are within a large cluster or network and, thus, are bulk-like (see Fig. S3). However, when the concentration is increased to 20m, the water molecules are more likely to exist in small water cluster domains, indicating that the system is too solvent-starved to form a bulk-like solvent structure. We further investigate Li^+ and $TFSI^-$ ionic clusters using the single-linkage clustering algorithm with a threshold distance of 0.30 nm, which corresponds to the first valley in the RDF from Li^+ ion to the oxygen atom in the $TFSI^-$ ion (see Fig. S4). As expected, the ions tend to form aggregated structures and the percentage of solvent separated single ions decreases with the increasing ion concentration. For the 20 m concentration, 15.9% and 8.4% of ions maintain solvent separated single ion and contact ion pair status, respectively. More than 70% of ions are in clusters composed of at least three ions (see Fig. S5). Remarkably, the largest ionic cluster/aggregate is composed of 6±2% of the total number of ions. This observation is generally consistent with the prior investigation.[8]

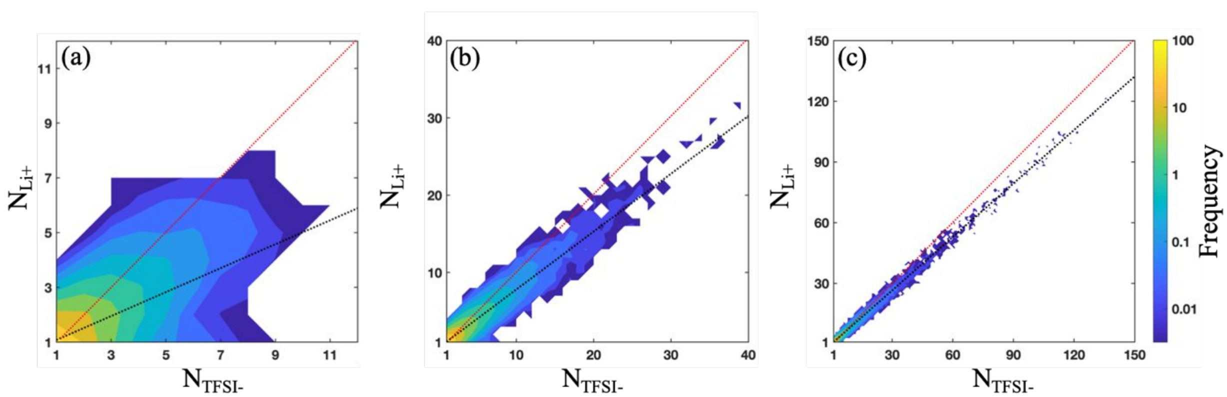

Figure 2. Time-averaged appearance freqeuncy map of number of ionic aggregates in (a) 10 m, (b) 15 m, and (c) 20 m LiTFSI aqueous electrolytes with specific number of $TFSI^-$ ion (N_{TFSI-}, *x*-axis) and Li^+ ion (N_{Li+}, *y*-axis). The color bar represents the occurrence frequency of the corresponding ionic aggregate with the corresponding anion and cation composition defined by the axises. The red diagonal line denotes neutrality, where $N_{TFSI-} = N_{Li+}$. The aggregates have positive charges above the line and negative charge below the line. The black dotted line was fit to the first-degree polynomials ($N_{Li+}=aN_{TFSI-}+b$, a and b fitting coefficient) and help guid the actual aggregate composition.

The composition of the ionic aggregates is further elucidated. As shown in Figure 2, the small aggregate composed of several ions is the most common case and the occurrence probability decreases with increasing aggregate size. For example, the fraction of aggregates with sizes containing less than 5 ions account for ~38% of the ionic aggregate population in the 20 m case.

The red dotted line in Figure 2 represents a symmetric composition of the ionic aggregate, which means an equal amount of cation and anion in the aggregate. We can see the distribution of aggregate composition fit to the first-degree polynomials (black dotted line) is below the red line in all three concentrations, meaning that more aggregates carry negative charges. The deviation from the symmetric composition is more prominent with larger aggregate sizes. Due to the overall system charge neutrality, negatively charged aggregates mean there will be Li^+-rich domains in the system. Indeed, the ratio of solvent separated single Li^+ ion and single $TFSI^-$ ion is 1.63 in the 20 m case. A ternary plot on the composition of the ternary aggregates composing of Li^+, $TFSI^-$, and water molecules has been shown in Figure S6. A representative snapshot of the largest water and ionic aggregates in 20 m LiTFSI in water is shown in Figure 3a to highlight the heterogeneous nanostructure and the distinct microscopic domains that form in this system. There are generally two regions in the electrolyte: an ionic aggregate domain with mostly salt composition and is relatively water-starved (blue and red in Figure 3a), and a domain that is relatively water-rich (shown in green in Figure 3a) and composed of some Li^+ ions.

Intuitively, ion aggregates should be neutral due to the electrostatic interaction between the Li^+ and $TFSI^-$ ions. A recent study on the PEO-LiTFSI system also indicates the existence of similar counterintuitive negatively charged clusters.[19] Nevertheless, the asymmetric aggregates don't always form in highly concentrated liquid electrolytes. For example, the sizes of the ionic aggregates are similar in 7 m LiTFSI acetonitrile electrolyte and 15 m LiTFSI aqueous electrolyte. However, the composition of the ionic aggregates in the former is more symmetric than latter (see Fig. S7a). When the concentration of LiTFSI increases to 12.5 m, almost all ions are connected with each other and mixed homogeneously with solvent molecules through the whole acetonitrile system. The other small ionic aggregates in this system also maintain charge neutrality (see Fig. S7b). This interesting difference between the aqueous and acetonitrile systems may originate from the higher binding energy between Li^+ and $TFSI^-$ ion in acetonitrile (i.e., -25.19 kcal/mol) than that (i.e., -20.12 kcal/mol) in water as calculated using Density Functional Theory. See supporting information for details of the binding energy calculations. The binding between Li^+ ion and acetonitrile or water is quite similar, with a binding energy of -15.62 and -15.40 kcal/mol, respectively. Therefore, the coordinated $TFSI^-$ ion around Li^+ in an aqueous electrolyte has higher tendency to be replaced by the solvent in the water system than in acetonitrile, which helps stabilize ion-separated domains in the aqueous system. In the dilute case, when there is enough solvent to fully solvate and stabilize the dissociated Li^+ ion, the salt dissociates to form separated ions and the solution is homogeneous; in the solvent-starved concentrated case, however, heterogeneous domains form in solution where the Li^+ ions can be stabilized in a water- and Li-rich domain while the anions form a relatively solvent-lean domain due to the limited total number of solvent. More in-depth studies on the thermodynamic drive for forming such nanometric asymmetric phases is however beyond the scope of this work.

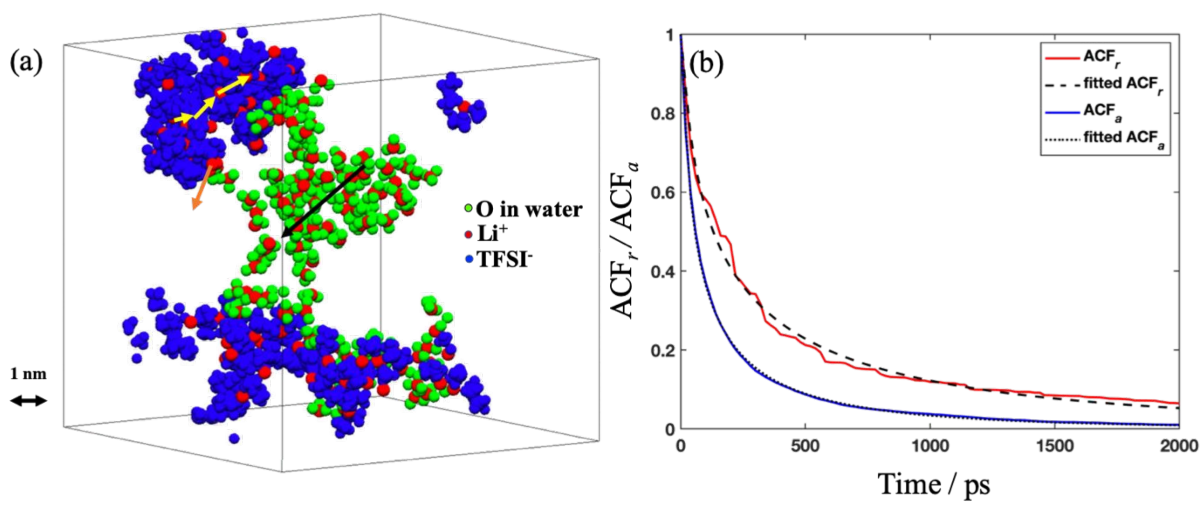

Figure 3. (a) A representative snapshot of the largest water and ionic aggregates in 20 m LiTFSI in water. The Li^+ diffusion mechanisms/paths in the different domains are also indicated with arrows. (b) Residence correlation function (ACF_r) for the aggregate and the Li-TFSI association correlation function (ACF_a). The two correlation functions are fitted to the stretched exponential function $\mathrm{ACF}(t)$

$= a_0 \exp\left(-\left({}^{t}/_{a_1}\right)^{a_2}\right)$, where a_0, a_1, and a_2 are fitting constants. The relaxation time constant of ACF (t) can be computed using $\tau = a_0 a_1 \Gamma\left(1 + {}^{1}/_{a_2}\right)$, where Γ is the gamma function.

The crosslinked heterogeneous ion and water domains in the highly concentrated aqueous electrolytes can play an important role in affecting the transport properties. For instance, nanometric water domains can benefit the diffusion of Li^+ ion[8, 9] and this diffusion mechanism is illustrated using a black arrow in Figure 3a. However, the transport mechanism of Li^+ ion in the ionic aggregate hasn't been reported. To characterize the dynamics of ions in the aggregate, we analyze the time scales for Li^+ ion dissociation from its neighboring anion within a aggregate (defined as association correlation function) and to escape from the aggregate (defined as residence correlation function). See supporting information for details of these definitions. From Figure 3b, we can see both correlation functions decay at a time scale on the order of nanoseconds. The relaxation time constant for the escape of Li^+ from the aggregate and from its associated $TFSI^-$ ion is 483.14 ps and 188.80 ps, respectively. This means the Li^+ ion can diffuse in the aggregate along the $TFSI^-$ ion (path shown in yellow arrows in Figure 3a) before leaving the aggregate and exchanging with Li^+ in the water-rich domain (orange arrow in Figure 3a). Furthermore, the self-part van Hove correlation function for Li^+ and $TFSI^-$ ion (see Fig. S8) shows that Li^+ ion has a longer tail in the 20 ps and 100 ps intervals, which means Li^+ ion in the aggregate has faster mobility compared to $TFSI^-$ ion in the aggregate. This observation suggests a hopping mechanism for Li^+ ion diffusion in the negative aggregate in the 20 m case. Therefore, there are three transport mechanisms of Li^+ ion in this heterogeneous structure. First, water separated single Li^+ ions can diffuse through the water domains. Second, Li^+ ions can diffuse along the anions within the aggregates. Third, Li^+ ions in the aggregates can exchange with Li^+ ions from the water domains.

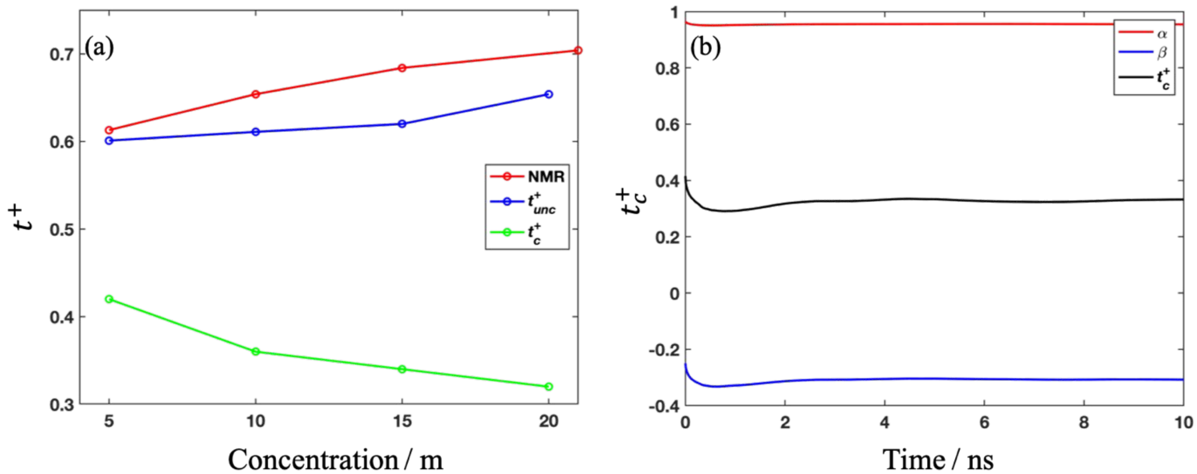

Figure 4. (a) The uncorrelated and correlation transference number (t^+_{unc}, t_c^+) calculated in the MD simulations and the transference number measured by pfg-NMR digitized from reference 8 (b) α, β, and t_c^+ changes with time.

The unique heterogeneous structure and transport mechanism described above in the WiSE electrolyte lead to an interesting behavior of the transference number. A high transference number of Li^+ ion represents a high fraction of the total current carried by Li^+ ion and implies high rate capability for the electrolyte. We calculated uncorrelated and correlated transference numbers (t^+_{unc}, t_c^+) for the WiSE. The t^+_{unc} ignores the correlation between the ions. Once the diffusion coefficient of all species is computed based on the diffusion regime in the mean square displacement, t^+_{unc} of species *i* equals to the ratio of diffusion coefficient of species *i* to the sum of all species. However, for the highly concentrated electrolytes including ionic liquid,[20, 21] solvate ionic liquid (SIL),[22] and polymer electrolyte, [23] high ion concentrations with strong electrostatic interactions lead to significantly correlated motion of the ions, which leads t^+_{unc} to deviate from the real scenario. Therefore, we also calculate the correlated transference number t_c^+ to compare with the traditional definition of t^+_{unc}. More simulation details can be found in the supporting information and some prior work.[22, 24] Two parameters (α, β) based on the Onsager coefficient ($\sigma_{++}, \sigma_{--}, \sigma_{+-}$) are used to compute t_c^+.[22, 24] The α is used to characterize which ion is more mobile and β represents the strength of the cation-anion dynamic correlation. Both strong positive correlation ($\beta \rightarrow 1$) and strong negative correlation ($\beta \rightarrow -1$) can reduce the t_c^+.[22, 24]

From Figure 4a, we can see t_{unc}^+ calculated using MD simulations is qualitatively consistent with those measured by pulsed-field gradient NMR.[8] That is the t_{unc}^+ increases with concentration moderately. This validates the force field for the investigation of the dynamic properties of these systems. However, t_c^+ decreases mildly with the concentration as shown in Figure 4b. This is because the ionic interaction and thus cation-anion dynamic correlation increases with the concentration. The t_c^+ is ~0.33 in 20 m, which is much higher than recent work on t_c^+ of equal molar LiTFSI and tetraglyme with a concentration of 4.5 m (i.e., ~0.06).[22] Furthermore, α and β (i.e., ~0.95 and ~-0.31) in our work are higher than those (i.e., ~0.56 and ~-0.87) calculated for the LiTFSI-in-tetraglyme.[22] If we change β from -0.87 in the LiTFSI-in-tetraglyme work to -0.31, the t_c^+ will change from 0.06 to 0.39, which is quite near the t_c^+ (i.e., ~0.33) in our work. This implies that the major difference on the t_c^+ between WiSE and LiTFSI-in-tetraglyme originates from the difference of β. In other words, the WiSE system has a relatively weaker negative correlation between the cation and anion. This is because, in the equal molar LiTFSI-in-tetraglyme electrolyte, there is no free solvent so the momentum conservation in the system dictates strong negative cation (i.e., $[Li(G4)]^+$)-anion (i.e., $TFSI^-$) correlation. On the contrary, in the WiSE system, there is a water-rich domain where Li^+ can move relatively free without a strong correlation with anions. On the other hand, it is important that the mass of the Li^+ ion plus the first water solvation shell (i.e., $[Li(H_2O)_n]^+$ n=0~4) is much less than $[Li(G4)]^+$, thus the anti-correlation is much weaker for WiSE despite much higher concentration compared to the LiTFSI-in-tetraglyme system.

In summary, we investigated the structure and dynamics of WiSE using MD simulations with experimentally validated force fields and discovered unique heterogeneous structure features and dynamic behaviors of the system. The simulations revealed percolating networks of negatively charged ion domains and positively charged water domains in the nanometric scale. The calculated t_c^+ in the 20 m WiSE is ~0.33, which is much higher than the recent reported t_c^+ (i.e., ~0.06) in the equal molar LiTFSI and tetraglyme electrolyte system. This comparison can be explained by the unique heterogeneous nanostructure of WiSE: although the dynamics of Li^+ ion in the ion domain is highly correlated in nature, the movement of the Li^+ in the water domain is relatively free. This is due to the small number of anions present in this domain, resulting in a weak overall correlation between ions and leading to a relatively high t_c^+ despite the high viscosity. Experimental SAXS data presented in this paper and previous pulsed-field gradient NMR studies[8] support our key simulation results on the formation of micro-domains and transport properties. This work provides us a fundamental understanding of the structure and dynamics of WiSE and also highlights the unique properties that could originate from the heterogeneities of a system.

Supporting information

The supporting information is available free of charge on the ACS publications website at DOI:

The MD simulation, analytical methods (e.g., structure factor calculation, single-linkage clustering algorithm, correlation function, and transference number), small angle X-ray scattering, RDFs between the oxygen atoms in the water molecules, cluster analysis of water moelcules, RDFs from the Li^+ ion to the oxygen atom in the $TFSI^-$ ion, the fraction of SSIPs, CIPs, and AGGs as a function of salt concentration, the cluster analysis of LiTFSI acetonitrile electrolytes, and self-part van Hove correlation function for Li^+ and $TFSI^-$ ion.

Acknowledgments

This research was supported by the Joint Center for Energy Storage Research (JCESR), a U. S. Department of Energy, Energy Innovation Hub. The submitted manuscript has been created by UChicago Argonne, LLC, Operator of Argonne National Laboratory ("Argonne"). Argonne, a U.S. Department of Energy Office of Science laboratory, is operated under Contract no. DE-AC02-06CH11357. This research used resources of the Advanced Photon Source, a U.S. Department of Energy (DOE) Office of Science User Facility operated for the DOE Office of Science by Argonne National Laboratory under Contract No. DE-AC02-06CH11357. We would acknowledge Dr. Oleg Borodin, Dr. Yong Zhang, Dr. Edward J. Maginn, Dr. Karina Shimizu, and Dr. Mingfei Zhao for helpful discussions. We thank the Laboratory Computing Resource Center at Argonne National Laboratory for generous allocation of computing time on the Bebop cluster.

Reference

(1) Huggins, R., Advanced batteries: materials science aspects. Springer Science & Business Media, 2008.

(2) Yu, Z. Molecular structure and dynamics of novel polymer electrolytes featuring Coulombic liquids. Virginia Tech, 2019.

(3) Li, W.; Dahn, J. R.; Wainwright, D. S., Rechargeable lithium batteries with aqueous electrolytes. *Science* **1994,** *264* (5162), 1115-1118.

(4) Scrosati, B.; Hassoun, J.; Sun, Y.-K., Lithium-ion batteries. A look into the future. *Energy Environ. Sci* **2011,** *4* (9), 3287-3295.

(5) Suo, L.; Borodin, O.; Gao, T.; Olguin, M.; Ho, J.; Fan, X.; Luo, C.; Wang, C.; Xu, K., "Water-in-salt" electrolyte enables high-voltage aqueous lithium-ion chemistries. *Science* **2015,** *350* (6263), 938-943.

(6) Suo, L.; Borodin, O.; Wang, Y.; Rong, X.; Sun, W.; Fan, X.; Xu, S.; Schroeder, M. A.; Cresce, A. V.; Wang, F., "Water-in-Salt" Electrolyte Makes Aqueous Sodium-Ion Battery Safe, Green, and Long-Lasting. *Adv. Energy Mater.* **2017,** *7* (21), 1701189.

(7) Leonard, D. P.; Wei, Z.; Chen, G.; Du, F.; Ji, X., Water-in-salt electrolyte for potassium-ion batteries. *ACS Energy Lett.* **2018,** *3* (2), 373-374.

(8) Borodin, O.; Suo, L.; Gobet, M.; Ren, X.; Wang, F.; Faraone, A.; Peng, J.; Olguin, M.; Schroeder, M.; Ding, M. S., Liquid structure with nano-heterogeneity promotes cationic transport in concentrated electrolytes. *ACS nano* **2017,** *11* (10), 10462-10471.

(9) Lim, J.; Park, K.; Lee, H.; Kim, J.; Kwak, K.; Cho, M., Nanometric Water Channels in Water-in-Salt Lithium Ion Battery Electrolyte. *J. Am. Chem. Soc.* **2018,** *140* (46), 15661-15667.

(10) Doherty, B.; Zhong, X.; Gathiaka, S.; Li, B.; Acevedo, O., Revisiting OPLS force field parameters for ionic liquid simulations. *J. Chem. Theory Comput* **2017,** *13* (12), 6131-6145.

(11) Jensen, K. P.; Jorgensen, W. L., Halide, ammonium, and alkali metal ion parameters for modeling aqueous solutions. *J. Chem. Theory Comput* **2006,** *2* (6), 1499-1509.

(12) Jorgensen, W. L.; Maxwell, D. S.; Tirado-Rives, J., Development and testing of the OPLS all-atom force field on conformational energetics and properties of organic liquids. *J. Am. Chem. Soc.* **1996,** *118* (45), 11225-11236.

(13) Jorgensen, W. L.; Chandrasekhar, J.; Madura, J. D.; Impey, R. W.; Klein, M. L., Comparison of simple potential functions for simulating liquid water. *J. Chem. Phys.* **1983,** *79* (2), 926-935.

(14) Li, T.; Senesi, A. J.; Lee, B., Small angle X-ray scattering for nanoparticle research. *Chem. Rev.* **2016,** *116* (18), 11128-11180.

(15) Feng, Z.; Sarnello, E.; Li, T.; Cheng, L., Communication—Microscopic View of the Ethylene Carbonate Based Lithium-Ion Battery Electrolyte by X-ray Scattering. *J. Electrochem. Soc.* **2019,** *166* (2), A47-A49.

(16) Shimizu, K.; Bernardes, C. E.; Triolo, A.; Lopes, J. N. C., Nano-segregation in ionic liquids: scorpions and vanishing chains. *Phys. Chem. Chem. Phys.* **2013,** *15* (38), 16256-16262.

(17) Kashyap, H. K.; Hettige, J. J.; Annapureddy, H. V.; Margulis, C. J., SAXS anti-peaks reveal the length-scales of dual positive–negative and polar–apolar ordering in room-temperature ionic liquids. *ChemComm* **2012,** *48* (42), 5103-5105.

(18) Shimizu, K.; Freitas, A. A.; Atkin, R.; Warr, G. G.; FitzGerald, P. A.; Doi, H.; Saito, S.; Ueno, K.; Umebayashi, Y.; Watanabe, M., Structural and aggregate analyses of (Li salt+ glyme) mixtures: the complex nature of solvate ionic liquids. *Phys. Chem. Chem. Phys.* **2015,** *17* (34), 22321-22335.

(19) Molinari, N.; Mailoa, J. P.; Kozinsky, B., Effect of Salt Concentration on Ion Clustering and Transport in Polymer Solid Electrolytes: A Molecular Dynamics Study of PEO–LiTFSI. *Chem. Mater.* **2018,** *30* (18), 6298-6306.

(20) Molinari, N.; Mailoa, J. P.; Craig, N.; Christensen, J.; Kozinsky, B., Transport anomalies emerging from strong correlation in ionic liquid electrolytes. *J. Power Sources* **2019,** *428*, 27-36.

(21) Molinari, N.; Mailoa, J. P.; Kozinsky, B., General Trend of Negative Li Effective Charge in Ionic Liquid Electrolytes. *J. Phys. Chem. Lett.* **2019,** *10* (10), 2313-2319.

(22) Dong, D.; Sälzer, F.; Roling, B.; Bedrov, D., How efficient is Li^+ ion transport in solvate ionic liquids under anion-blocking conditions in a battery? *Phys. Chem. Chem. Phys.* **2018,** *20* (46), 29174-29183.
(23) Fong, K. D.; Self, J.; Diederichsen, K. M.; Wood, B. M.; McCloskey, B. D.; Persson, K. A., Ion Transport and the True Transference Number in Nonaqueous Polyelectrolyte Solutions for Lithium Ion Batteries. *ACS Cent. Sci.* **2019,** *5*, (7), 1250-1260.
(24) Wohde, F.; Balabajew, M.; Roling, B., Li^+ transference numbers in liquid electrolytes obtained by very-low-frequency impedance spectroscopy at variable electrode distances. *J. Electrochem. Soc.* **2016,** *163* (5), A714-A721.